第 24 卷第 9 期 无 机 化 学 学 报 Vol.24 No.9
2008 年 9 月 CHINESE JOURNAL OF INORGANIC CHEMISTRY 1387~1392

生物分子 *L*-半胱氨酸辅助的六角形 γ-硫化锰的水热合成与表征

郭培志*,[1] 李洪亮[1] 于建强[1] 孙 红[1] 赵修松*,[1,2]
([1]青岛大学化学化工与环境学院,纤维新材料与现代纺织国家重点实验室培育基地,青岛 266071)
([2]Department of Chemical and Biomolecular Engineering, National University of Singapore,
4 Engineering Drive 4, Singapore 117576, The republic of Singapore)

摘要:本文使用 *L*-半胱氨酸和不同类型的锰盐通过水热方法合成了具有不同直径和长度的六角形 γ-硫化锰的单晶纳米棒,并通过 X-射线衍射、扫描电子显微镜和透射电子显微镜实验对 γ-硫化锰纳米棒的结构和性质进行了表征。实验结果表明不同锰盐中的阴离子对六角形 γ-硫化锰纳米棒的形成具有影响并对其形成机理进行了简单讨论。

关键词:γ-硫化锰; *L*-半胱氨酸; 纳米棒; 单晶
中图分类号:O613.5; O614.7 **文献标识码**:A **文章编号**:1001-4861(2008)09-1387-06

Hydrothermal Synthesis and Characterization of Hexagonal γ-MnS Single Crystal Nanorods in Presence of Biomolecule *L*-cysteine

GUO Pei-Zhi*,[1] LI Hong-Liang[1] YU Jian-Qiang[1] SUN Hong[1] ZHAO Xiu-Song*,[1,2]
([1]*Laboratory of New Fiber Materials and Modern Textile, Growing Base for State Key Laboratory, School of Chemistry, Chemical Engineering and Environmental Sciences, Qingdao University, Qingdao* 266071)
([2]*Department of Chemical and Biomolecular Engineering, National University of Singapore*, 4 *Engineering Drive* 4 *Singapore* 117576, *The Republic of Singapore*)

Abstract: Hexagonal γ-MnS nanorod crystals of different diameters and length scales were hydrothermally synthesized in the presence of biomolecule *L*-cysteine and Mn(Ⅱ) salts, and characterized by X-ray powder diffraction (XRD), scanning electron microscopy (SEM) and transmission electron microscopy (TEM). The effects of different anions on the formation of hexagonal γ-MnS nanorods were discussed to show the importance of a precursor in synthesizing such nanomaterials.

Key words: γ-MnS; *L*-cysteine; nanorod; single crystal

One-dimensional(1D) nanostructured materials are receiving growing attention because of their unique optical, electronic and magnetic properties for applications as nanodevices[1~3]. Especially, 1D semiconductor nanomaterials are important building blocks for fabrication of active and integrated nanodevices. So far, various methods for the preparation of 1D nanomaterials have been reported[3~6].

As a ⅦB-ⅥA semiconductor, manganese sulfide (MnS) with a band gap energy of 3.2 eV at room temperature has potential applications in solar cells as window/buffer materials, short wavelength optoelectronic materials and diluted magnetic semiconductors (DMS)[7~10]. Crystallographically, MnS can exist in three forms: the stable green α-MnS with a rock-salt structure and two metastable tetrahedral structures, namely, the spha-

收稿日期:2008-01-07。收修改稿日期:2008-06-01。
国家自然科学基金(No.50602028)青岛大学引进人才基金和胶体与界面化学教育部重点实验室(山东大学)开放课题项目资助。
*通讯联系人。E-mail:pzguo@qdu.edu.cn; chezxs@nus.edu.sg
第一作者:郭培志,男,31 岁,博士,副教授;研究方向:微纳材料结构与性能。

lerite β-MnS and wurtzite γ-MnS[11]. Upon heating, both of the two metastable phases can be transformed irreversibly to stable α-MnS [12,13]. The synthesis of MnS nanocrystals, thin films, spheres and hollow shperes has been described [9,10,14~19]. 1D MnS nanostructures were also reported in the above cited literatures, these 1D MnS nanostructures could be synthesized using thermolysis[19], template synthesis[20], solvothermal and hydrothermal synthesis[21~23] and chemical vapour deposition(CVD) methods [24,25]. It has been reported that the sulfur source plays a key role in forming nanostructured MnS materials[18,26]. On the other hand, the counter anion of metal salts has also been observed to play a role in the formation of MnS nanostructures due to the complicated nature of the hydrothermal synthesis[27,28]. Although the synthesis of hexagonal wurtzite MnS nanocrystals has been described [29], the synthesis of hexagonal γ-MnS nanorod and nanowire single crystals has not been reported to the best of our knowledge.

Biomolecule-assisted synthesis is believed to afford controllable properties of the resultant nanostructures[18,30,31]. For example, glutathione has been employed as both sulfur source and assembling molecule to synthesize novel hierarchical nanostructures of Bi_2S_3 under hydrothermal conditions[31]. Recently, metastable γ-MnS porous networks have been synthesized using biomolecule *L*-cysteine[18]. The functional groups, -SH, -COOH and $-NH_2$, in the cysteine molecule were found to play a crucial role in the synthesis of the porous MnS structures [18]. However, the fine regulation of the effects of the counter anions is still an interesting subject in the controllable fabrication of MnS nanostructures. In this work, we experimentally examined the effect of different Mn(Ⅱ) salts, including $Mn(NO_3)_2$, $MnSO_4$, and $Mn(CH_3COO)_2$, on the formation of γ-MnS nanostructure in a hydrothermal system in the presence of biomolecule *L*-cysteine. The formation mechanism of γ-MnS nanorods was also discussed.

1 Experimental

All chemicals, including alcohols, $Mn(NO_3)_2$(aqueous solution, 50%), $MnSO_4 \cdot H_2O$, $Mn(CH_3COO)_2 \cdot 4H_2O$, and *L*-cysteine were of analytical grade and used without further purification. In a typical synthesis, aqueous $Mn(NO_3)_2$ solution (1.07 g, 3 mmol), distilled water (30 mL) and *L*-cysteine(C_3H_7NS)(0.363 g, 3 mmol) were mixed under stirring. After 5 min, the mixture was transferred to a 40 mL teflon-lined autoclave. Hydrothermal synthesis was carried out in an oven at 150 ℃ for 24 h. The solid was collected and washed with distilled water and absolute ethanol, dried in an oven at 60 ℃ for 6 h. The molar ratio of Mn over S in all synthesis recipes was 1 unless otherwise specified.

X-ray powder diffraction(XRD) measurements were determined using a Bruker D8 advanced X-ray diffractmeter equipped with graphite monochromatized Cu $K\alpha$ radiation(λ=0.154 18 nm) and Ni filter from 10° to 80° (2θ) and operated at 40 kV and 40 mA. Scanning electron microscopy(SEM) images were taken with a JSM-6390LV scanning electron microscope operated at 20 kV. Transmission electron microscopy(TEM) images were obtained with a JEM-2000EX transmission electron microscope operated at 160 kV with the distance of 80.0 cm for electron diffraction.

2 Results and discussion

Pink solids were obtained when $MnSO_4$ and $Mn(NO_3)_2$ were used as Mn sources and the synthesis temperature was 150 ℃, but dark red solids were harvested under all other experimental conditions. The powder X-ray diffraction (XRD) patterns of the solid products synthesized using different Mn(Ⅱ) salts are shown in Fig.1. The diffraction peaks of the precipitates in Fig.1A, C and F can be clearly indexed to hexagonal γ-MnS phase(PDF 40-1289) from the *L*-cysteine systems with $Mn(NO_3)_2$, $MnSO_4$ and $Mn(CH_3COO)_2$ at 150 ℃, respectively. The sharp diffraction peaks reveal a good crystallinity of the metastable γ-MnS phase in the products.

When the synthesis temperature is increased to 180 ℃, the main peaks of hexagonal γ-MnS phase are still seen from the XRD patterns of the samples using $Mn(NO_3)_2$ and $Mn(CH_3COO)_2$ as the Mn precursor, as shown in Fig.1B and G, respectively. However, two obvious peaks with the 2θ values of 34.50° and 49.30° can be observed for the MnS samples from the $MnSO_4$ and

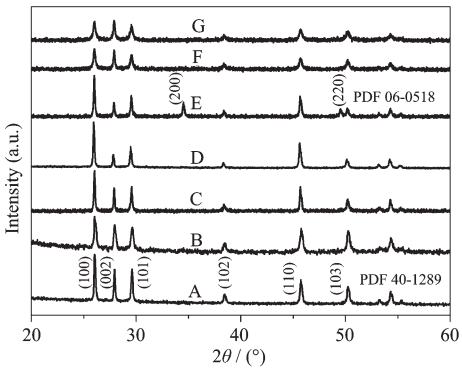

Fig.1　XRD patterns of the MnS nanostructures, synthesized from the *L*-cysteine systems for 24 h with $Mn(NO_3)_2$[150 ℃, (A), 180 ℃, (B)], $MnSO_4$[150 ℃, (C), 180 ℃, (D), 8h; E, (PDF 06-0518)] and $Mn(CH_3COO)_2$ [150 ℃, (F), 180 ℃, (G)]

L-cysteine systems at 180℃ for 24 h (Fig.1E), which can be ascribed to(200) and(220) peaks of α-MnS phase (PDF 06-0518), respectively, indicating that the synthesizing temperature played a crucial rule on the formation of pure MnS phases. Furthermore, no obvious peaks of α-MnS phase can be found for the same systems if the reaction time was 8 h(Fig.1D). These results indicated that the phase transition of γ-MnS to α-MnS was occured during the hydrothermal reaction process with the temperature up to 180 ℃. And the anions of Mn(Ⅱ) salts could indeed contribute to the phase transition of γ-MnS to α-MnS as the transition temperatures maybe different for the studied *L*-cysteine systems[18]. If the temperature was increased to more than 200 ℃, the pure α-MnS phase can be obtained[8,18].

Fig.2 shows the typical SEM images of the MnS products. It can be seen that uniform hexagonal γ-MnS nanorods with diameters of 300~500 nm and lengths up to over ten micrometers are formed using the $Mn(NO_3)_2$ and *L*-cysteine systems at 150 ℃(Fig.2A). At the same synthesis temperature, the use of $MnSO_4$ as the Mn source leads to MnS nanorods with a larger diameter (500 ~800 nm) and a longer length (up to 15 μm) as shown in Fig.2C. When $Mn(CH_3COO)_2$ is used, however, sphere aggregates of small hexagonal MnS nanorods of about 100 nm in diameter and 300~1 000 nm in length can be obtained(Fig.2E). It has been reported that tortuous wire-like γ-MnS nanostructures and the γ-MnS porous networks with small amount α-MnS phase are obtained using $MnCl_2$ in the presence of *L*-cysteine at the temperatures between 120 ℃ and 150 ℃[18]. According to our experimental data, pure hexagonal γ-MnS nanorods are formed at 150 ℃, while the morphology of the resultant MnS nanostructures is changed greatly with the temperature up to 180 ℃. Disordered aggregates instead of nanorods are observed for the $Mn(NO_3)_2$ systems(Fig.2B), while the contracted nanospheres composed of disordered nanoparticles are observed from the $Mn(CH_3COO)_2$ systems (Fig.2F). Simi-

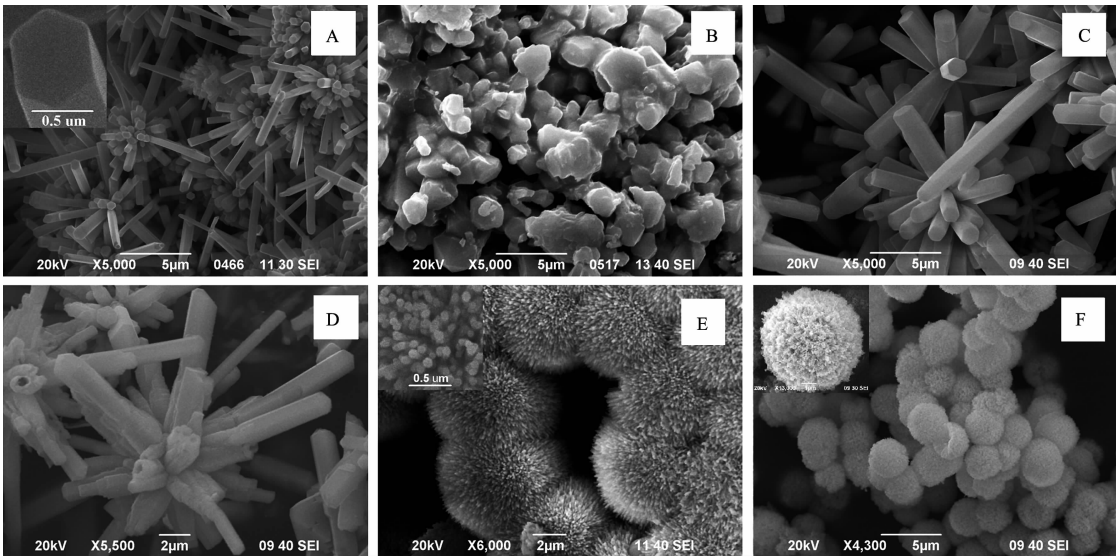

Fig.2　Typical SEM images of the as-prepared γ-MnS structures from the homogeneous *L*-cysteine systems with $Mn(NO_3)_2$(A and B), $MnSO_4$(C and D) and $Mn(CH_3COO)_2$(E and F). The synthesis temperature of samples A, C, and E is 150 ℃ and the left(B, D, F) is 180 ℃

larly, no characteristic nanostructures are formed for the $MnSO_4$ system, in which the phase transition of α-MnS to γ-MnS is occured obviously (Fig.2D). These results further show that different counter-anions in Mn(Ⅱ) salts and the reaction temperatures play important roles in controlling the ultimate MnS nanostructures.

Fig.3 shows typical TEM images and SAED patterns of the metastable MnS nanostructures. Fig.3A~B show the γ-MnS nanorod crystals with about 500 nm in diameter and 3~5 μm in length synthesized using $Mn(NO_3)_2$ and $MnSO_4$ as Mn sources, respectively. The occurrence of the side edges in the up head of the nanorods confirmed the hexagonal nature of the synthesized nanostructures. For the γ-MnS nanostructures fabricated from $Mn(CH_3COO)_2$ systems, the side length is decreased to ~100 nm and the nanorods could be extended to several hundred nanometers. These results are in good agreement with the SEM data. From the SAED patterns shown in the insets of Fig.3A~C, the nanorod can be identified as the[110] zone axis projection of the reciprocal lattice of γ-MnS phase. And it can be concluded that the rods grow along the *c* direction of the MnS lattice. This orientation of the γ-MnS nanorods should be similar to those of hexagonal wurtzite CdSe nanorods[32]. Under the hydrothermal condition at 180 ℃, the growth of the metastable γ-MnS nanostructures may be kinetically driven and the crystal phase transition of γ-MnS to α-MnS is occurred. Consequently, the MnS nanorod single crystals can not be formed and disordered nanoparticles are observed for all the systems(Fig.3D~F).

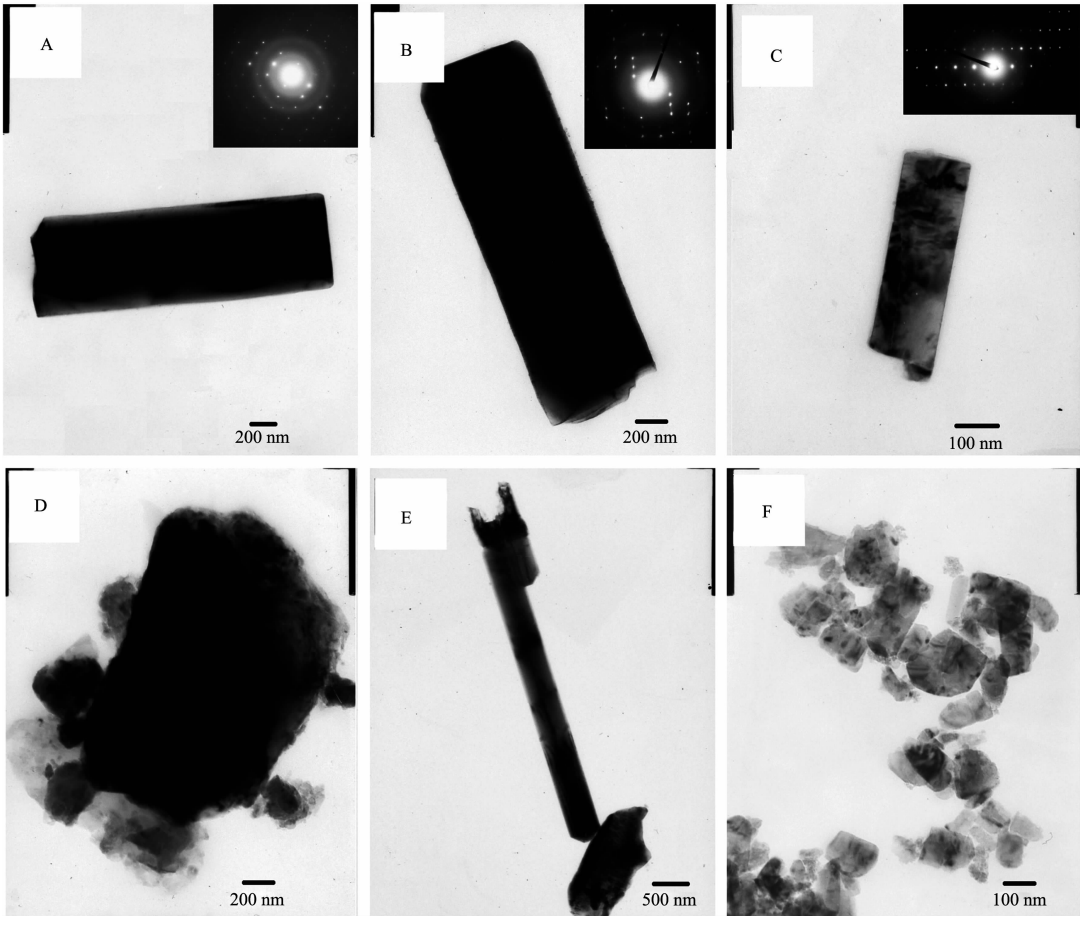

Fig.3 Typical TEM images of the as-prepared γ-MnS nanostructures from the homogeneous *L*-cysteine systems with $Mn(NO_3)_2$ (A and D), $MnSO_4$ (B and E) and $Mn(CH_3COO)_2$ (C and F). The reaction temperature of samples A, B, and C is 150 ℃ and D, E, F is 180 ℃.

Fig.4 shows the SEM images of the γ-MnS nanostructures of $Mn(NO_3)_2$ systems with different molar ratios of Mn to S at 150 ℃. It can be seen that the hexagonal nanorods with the n_{Mn}/n_S ratio of 2∶1(Fig.4A) are almost the same as those of the n_{Mn}/n_S ratio of 1∶1. However, the morphology changes to somewhat irregular nanostruc-

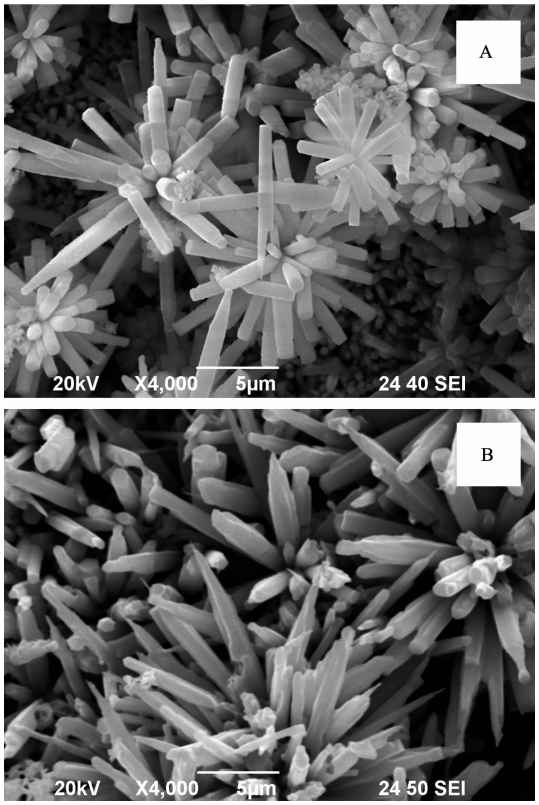

Fig.4　SEM images of the as-prepared MnS nanostructures from the $Mn(NO_3)_2$ and *L*-cysteine system at 150 ℃ with the molar ratios of Mn to S being 2:1(A) and 1:2(B)

tures obtained from the n_{Mn}/n_S ratio of 1:2(Fig.4B). These results indicate that the molar ratio of $Mn(NO_3)_2$ to *L*-cysteine has strong effect on the coordination of Mn(Ⅱ) and the functional groups of *L*-cysteine[18], and the coordination have contribution to the resultant MnS nanostructures.

As the *L*-cysteine molecule contains three functional groups, -SH, -COOH and $-NH_2$, metal ions have the strong tendency to coordinate with such groups[33]. From the results above and reported in the literature[18], it is no doubt that the formation of these hexagonal nanostructures is relevant to the coordination interaction between Mn(Ⅱ) ions, counter anions and *L*-cysteine molecules. To further investigate the mercapto group on the fabrication of MnS nanostructures, the racemic methionine molecules are used in our experiments and no precipitate can be observed even if the reaction temperature is increased to 200 ℃. And no rod-like structures can be found also if the tetrahydrothiophene is used as the sulphur source.

The experimental data also show that the anions of Mn(Ⅱ) salts affect the morphology of the γ-MnS nanostructures. According to Ref.[18], tortuous γ-MnS nanowires are formed when $MnCl_2$ is used. Hexagonal γ-MnS nanorods are obtained when the anions become NO_3^-, SO_4^{2-}, or CH_3COO^- at the otherwise identical synthesis conditions. Furthermore, the diameter and length scales of the γ-MnS nanorod crystals are gradually increased with the order of CH_3COO^-, NO_3^-, and SO_4^{2-} ions. These indicate that the nature of different anions could contribute to the formation of the γ-MnS nanostructures, similar to other metal sulfide nanomaterials.[28] It is suggested that the CH_3COO^- ions has strong coordination ability with the metal ions leading to the formation of smaller sized hexagonal γ-MnS nanorods. And it is also suggested that one Mn(Ⅱ) ion may coordinate with one *L*-cysteine molecule to form the hexagonal nanorod crystals. This preassumption can be supported by the results through changing the molar ratios and that hexagonal γ-MnS nanocrystal could be formed through the reaction of $MnCl_2$ and element sulfur in oleylamine with the molar ratio of 3∶1 as reported by Hyeon et al[29]. In our experiments, the straight hexagonal γ-MnS nanorods can also be obtained with the molar ratio of Mn over S in the raw materials higher than 1.

3　Conclusions

Hexagonal γ-MnS nanorod crystals with different diameters and length scales were synthesized by a *L*-cysteine-assisted hydrothermal synthesis method through changing the Mn(Ⅱ) salts. And the counter ions of Mn(Ⅱ) salts are contributed to the formation of the different γ-MnS nanorods, showing the importance of a precursor in synthesizing nanostructures. Furthermore, the crystal phase transition of γ-MnS to α-MnS can be detected and irregular nanoparticles are formed with the temperature increased.

References:

[1] Duan X F, Huang Y, Agarwal R, et al. *Nature*, **2003**,**421**:241~245

[2] Park W I, Jun Y, Jung, S W, et al. *Appl. Phys. Lett*., **2003**,**82:**

964~966

[3] Xia Y N, Yang P D, Sun Y G, et al. *Adv. Mater.*, **2003**,**15**: 353~398

[4] Hou S, Wang J, Martin C. R. *J. Am. Chem. Soc.*, **2005**,**127**: 8586~8587

[5] Lu W, Xiang J, Timko B P, et al. *Proc. Natl. Acad. Sci.*, **2005**, **102**:10046~10051

[6] Lauhon L J, Gudiksen M S, Wang D, et al. *Nature*, **2002**,**420**: 57~61

[7] Furdyna J K. *J. Appl. Phys.*, **1998**,**64**:R29

[8] Goede O, Heimbrodt W. *Phys. Stat. Sol. B*, **1988**,**146**:11~62

[9] Lei S J, Tang K B, Yang Q, et al. *Eur. J. Inorg. Chem.*, **2005**, 4124~4128

[10]Fan D B, Yang X D, Wang H, et al. *Physica B*, **2003**,**337**: 165~169

[11]Pajaczkowska A, Rabenaut A. *J. Solid State Chem.*, **1977**,**21**: 43~48

[12]Kennedy S W, Harris K, Summerville E. *J. Solid State Chem.*, **1980**,**31**:355~359

[13]Biswas S, Kar S, Chaudhuri S. *J. Cryst. Growth*, **2005**,**284**: 129~135

[14]Cheng Y, Wang Y S, Jia C, et al. *J. Phys. Chem. B*, **2006**,**110**: 24399~24402

[15]Amirav L, Lifshitz E. *J. Phys. Chem. B*, **2006**,**110**:20922~20926

[16]Gumus C, Ulutas C, Esen R, et al. *Thin Solid Films*, **2005**, **492**:1~5

[17]Tao F, Wang Z J, Yao L Z, et al. *Mater. Lett.*, **2007**,**61**:4973~4975

[18]Zuo F, Zhang B, Tang X Z, et al. *Nanotechnology*, **2007**,**18**: 215608

[19]Jun Y W, Jung Y Y, Cheon J. *J. Am. Chem. Soc.*, **2002**,**124**: 615~619

[20]Zhang C, Tao F, Liu G Q, et al. *Mater. Lett.*, **2008**,**62**,246~248

[21]An C, Tang K, Liu X, et al. *J. Cryst. Growth*, **2003**,**252**:575~580

[22]Lu J, Qi P, Peng Y, et al. *Chem. Mater.*, **2001**,**13**:2169~2172

[23]Zheng Y H, Cheng Y, Wang Y S, et al. *J. Phys. Chem. B*, **2006**,**110**:8284~8288

[24]Kim D S, Lee J Y, Na C W, et al. *J. Phys. Chem. B*, **2006**,**110**: 18262~18266

[25]Ge J P, Li Y D. *Chem. Commun.*, **2003**,2498~2499

[26]Liu Z P, Liang J B, Li S, et al. *Chem. Eur. J.*, **2004**,**10**:634~640

[27]Yao W T, Yu S H. Int. *J. Nanotechnology*, **2007**,**4**:129~162

[28]Ni Y H, Wei X W, Hong J M, et al. *Mater. Res. Bull.*, **2007**,**42**:17~26

[29]Joo J, Na H B, Yu T, et al. *J. Am. Chem. Soc.*, **2003**,**125**: 11100~11105

[30]Zhang L, Gaponik N, Muller J, et al. *Small*, **2005**,**1**:524~527

[31]Lu Q Y, Gao F, Komareni S. *J. Am. Chem. Soc.*, **2004**,**126**: 54~55

[32]Peng X G, Manna L, Yang W D, et al. *Nature*, **200**0,404:59~61

[33]Zhang W W, Lu C S, Zou Y, et al. *J. Coll. Interf. Sci.*, **2002**, **249**:301~306